Inflammation Research (2022) 71:1079–1094
https://doi.org/10.1007/s00011-022-01620-z

Inflammation Research

ORIGINAL RESEARCH ARTICLE

STAT1-mediated induction of Ly6c-expressing macrophages are involved in the pathogenesis of an acute colitis model

Shuhei Kii[1,2] · Hidemitsu Kitamura[1] · Shinichi Hashimoto[3] · Kazuho Ikeo[4] · Nobuki Ichikawa[2] · Tadashi Yoshida[2] · Shigenori Homma[2] · Mishie Tanino[5] · Akinobu Taketomi[2]

Received: 27 September 2021 / Revised: 28 June 2022 / Accepted: 16 July 2022 / Published online: 1 August 2022

Abstract

Background The development of inflammatory bowel diseases is thought to be multifactorial, but the exact steps in pathogenesis are poorly understood. In this study, we investigated involvement of the activation of STAT1 signal pathway in the pathogenesis of an acute colitis model.

Methods A dextran sulfate sodium-induced acute colitis model was established by using wild-type C57BL/6 mice and STAT1-deficient mice. Disease indicators such as body weight loss and clinical score, induction of cytokines, chemokines, and inflammatory cells were evaluated in the acute colitis model.

Results Disease state was significantly improved in the acute colitis model using STAT1-deficient mice compared with wild-type mice. The induction of Ly6c-highly expressing cells in colorectal tissues was attenuated in STAT1-deficient mice. IL-6, CCL2, and CCR2 gene expressions in Ly6c-highly expressing cells accumulated in the inflamed colon tissues and were significantly higher than in Ly6c-intermediate-expressing cells, whereas TNF-α and IFN-α/β gene expression was higher in Ly6c-intermediate-expressing cells. Blockade of CCR2-mediated signaling significantly reduced the disease state in the acute colitis model.

Conclusions Two different types of Ly6c-expressing macrophages are induced in the inflamed tissues through the IFN-α/β-STAT1-mediated CCL2/CCR2 cascade and this is associated with the pathogenesis such as onset, exacerbation, and subsequent chronicity of acute colitis.

Keywords Signal transducer and activator of transcription 1 · CCR2 · Ly6c · Macrophages · Inflammatory bowel disease

Introduction

Inflammatory bowel diseases (IBDs), such as ulcerative colitis (UC) and Crohn's disease (CD), are chronic, relapsing, and remitting inflammatory disorders of the gut. The number of IBD patients has increased all over the world [1, 2]. However, the exact steps of pathogenesis, including onset, exacerbation, and the subsequent chronicity, are poorly understood because the development of IBD has been thought to be multifactorial [3, 4]. The gut microbiota that is composed

Responsible Editor: John Di Battista.

✉ Hidemitsu Kitamura
kitamura@igm.hokudai.ac.jp

Kazuho Ikeo
kikeo@nig.ac.jp

Shigenori Homma
homma.s@nifty.com

Mishie Tanino
mtanino@asahikawa-med.ac.jp

Akinobu Taketomi
taketomi@med.hokudai.ac.jp

[1] Division of Functional Immunology, Section of Disease Control, Institute for Genetic Medicine, Hokkaido University, Sapporo, Japan

[2] Department of Gastroenterological Surgery I, Hokkaido University Graduate School of Medicine, Sapporo, Japan

[3] Department of Molecular Pathophysiology, Institute of Advanced Medicine, Wakayama Medical University, Wakayama, Japan

[4] DNA Data Analysis Laboratory, National Institute of Genetics, Mishima, Japan

[5] Department of Surgical Pathology, Asahikawa Medical University, Asahikawa, Japan

of bacteria, yeasts, fungi, and viruses have been implicated in IBD [5–9]. Recent researches have shown the gut virome alterations in IBD patients [10–12]. Therefore, infection by viruses and bacteria and the resulting composition of gut microbes may play a role in disease pathogenesis and the degree of severity in patients with IBD. During the pathogenesis of IBD, innate immune cells such as macrophages and dendritic cells directly drive intestinal inflammation by releasing large amounts of inflammatory cytokines, such as tumor necrosis factor (TNF)-α, and interleukin (IL)-6, IL-12, or IL-23 [13–18].

Interferons (IFNs), typically classified as Type I, Type II, and Type III, are produced by host cells in response to viral infections. Members of the signal transducer and activator of transcription (STAT) protein family are intracellular transcription factors that mediate many aspects of cellular immunity, proliferation, apoptosis, and differentiation [19]. They are primarily activated by membrane receptor-associated Janus kinases. When Type-I IFNs, IFN-α/β, and/or Type II IFN, IFN-γ, bind to the receptor, STAT1 is activated. In general, IFN-α/β is produced by innate myeloid-type immune cells and fibroblasts, and IFN-γ is produced by natural killer (NK) cells, NKT cells, and T cells [20, 21].

Several experimental models reveal the relevance of STAT1 activation in the onset and progression of colitis. Previous research demonstrated that dextran sulfate sodium (DSS) treatment affected wild-type mice (WT mice) more than STAT1 knockout mice (KO mice) and phylotype-level 16S rRNA analysis revealed bacterial indicators of the health state in acute murine colitis [22]. Immunological and protective effects were observed in an acute DSS-induced colitis mouse model with conditional deletion of STAT1 in the intestinal epithelium [23]. A recent study revealed a role for STAT1 in enabling T cells to induce colitis by protecting them from NK cell-mediated cytotoxicity [24]. The IFN-γ-STAT1 signaling pathway was reported to be required for generating colitogenic macrophages, based on the finding that STAT1 KO mice had less severe colitis and fewer colitogenic macrophages [25]. Selective sequestration of STAT1 in the cytoplasm via phosphorylated SHP-2, ameliorates murine experimental colitis [26]. Hyaluronan-mediated leukocyte adhesion and DSS-induced colitis were attenuated in the absence of STAT1 [27]. It is reported that increased STAT1 activation is observed in monocytes and neutrophils in the inflamed mucosa of IBD patients [28]. However, details of relationship between STAT1 activation and pathogenesis of IBD, including onset, exacerbation, and the subsequent chronicity have not been fully elucidated. Therefore, we investigated the induction mechanism of colitogenic macrophages and the involvement of the STAT1 signal pathway and regulating factors in the onset of colitis.

In this study, we found that DSS-induced acute colitis was attenuated in STAT1 KO mice and that Type I IFNs, IFN-α/β, proinflammatory cytokines, IL-6/TNF-α, and chemokines, CCL2/CCR2, are induced in two different types of Ly6c-expressing macrophages triggering the development of a colitis model in a STAT1-dependent manner. These findings reveal that the Type I IFN/STAT1–CCL2/CCR2 axis in colitogenic macrophages is associated with the initial steps of colitis, suggesting a promising target to prevent the onset, exacerbation, and subsequent chronicity of IBD in patients.

Materials and methods

Reagents and antibodies

The following monoclonal antibodies were obtained from BioLegend (San Diego, CA, USA) or BD Biosciences (San Diego, CA, USA): fluorescent dye-conjugated anti-CD45 (30-F11), anti-Ly6c (HK1.4), anti-CD11b (M1/70), anti-CD11c (N418), anti-I-A^d (AF6-120.1), anti-CD4 (GK1.5), anti-CD8 (53–6.7), and Gr-1 (RB6-8C5). 7-AAD Viability Dye was purchased from Beckman Coulter (Marseille Cedex, France). Recombinant murine IFN-α (752,802) and IFN-β (581,302) were purchased from BioLegend. Recombinant murine IFN-γ was purchased from Peprotech Inc. (Rocky Hill, NJ, USA) and lipopolysaccharide (LPS) was from Sigma-Aldrich Co. (St Louis, MO, USA). CCR2 antagonist (RS504393) was purchased from Abcam (Cambridge, United Kingdom).

Mice

Wild-type C57BL/6 female mice were obtained from Charles River Japan (Kanagawa, Japan). STAT1 KO mice were first established by Dr. R.D. Schreiber (Washington University, MO, USA). C57BL/6 background STAT1 KO mice were established by backcrossing with WT C57BL/6 mice eight times. All mice were maintained in specific-pathogen-free conditions according to the guidelines of the animal department at Hokkaido University and were used at 6–8 weeks of age.

All mouse experiments were approved by the Animal Ethics Committee of Hokkaido University (No. 14-0039, 19-0035, 19-0065) and were conducted in accordance with the recommendations in the Guide for the Care and Use of Laboratory Animals of the University.

Human subjects

Two active UC patients (Pt#1, severe, Matts grade 4; Pt#2, moderate, Matts grade 3) who underwent surgery at Hokkaido University Hospital were included in this study. Patients were followed up at 1- to -6-month intervals until

March 31, 2018, or death. Research protocols involving human subjects were approved by the institutional review board of Hokkaido University Graduate School of Medicine (14-043) and the Institute for Genetic Medicine (14-0004). Written informed consent was obtained from each patient. All procedures in this study were carried out in accordance with the relevant guidelines and regulations and according to the Declaration of Helsinki.

Cell culture

Spleen cells and peritoneal exudate cells from wild-type and STAT1 KO mice were maintained in RPMI-1640 medium (FUJIFILM Wako Pure Chemical Industries, Ltd., Osaka, Japan) supplemented with 10% fetal calf serum, 100 µg/ml streptomycin, 200 U/ml penicillin, 10 mM HEPES, and 0.05 mmol/l 2-mercaptoethanol (Sigma-Aldrich, Tokyo, Japan) at 37 °C in 5% CO_2. For flow cytometry, spleen cells (2.0×10^6) or PECs (5.0×10^5) were cultured in 12-well culture plates and treated with IFN-α, IFN-β, or IFN-γ (50 ng/ml) for 24 h.

Bone marrow cells were prepared from wild-type and STAT1 KO mice. Bone marrow-derived dendritic cells (BMDCs) were induced in 12-well culture plates in the presence of GM-CSF for 6 days as previously reported [29]. The WT and STAT1-deficient BMDCs were stimulated with IFN-β (50 ng/ml) or LPS (100 ng/ml) for 3 h or 6 h, respectively.

An acute colitis model

To induce experimental colitis, the female mice received 3% (w/v) DSS (FUJIFILM Wako Pure Chemical Corporation, Osaka, Japan) in their drinking water that was provided ad libitum for 7 days. Weight measurements were performed daily. The mice were euthanized on day 7 or day 10 and their large intestines were collected without the cecum as described previously [30]. Briefly, the colon was removed, cut longitudinally, and washed in PBS. Paraffin sections were stained with HE. Histological scoring was performed in a double-blind fashion by two investigators. The severity of the colitis was assessed according to the scoring system, as described previously [31]. The grading index was as follows: inflammation severity (0: none, 1: mild, 2: moderate, and 3: severe), inflammation extent (0: none; 1: mucosa, 2: mucosa and submucosa, and 3: transmural), crypt damage (0: none, 1: one-third of the basal tissue damaged, 2: two-thirds of the basal tissue damaged, 3: only the surface epithelium intact, and 4: the entire crypt and epithelium is lost), and the percentage involved in the ulcer or erosion (1: < 1%, 2: 1–15%, 3: 16–30%, 4: 31–45%, and 5: 46–100%). The sum of the first three scores (severity, extent, and crypt damage) was multiplied by the percentage involvement score to obtain the final value for comparison. These scores were evaluated for the distal colon, the middle colon, and the proximal colon.

PCR analysis

Total RNA was extracted using ISOGEN (Nippon gene, Toyama, Japan) according to the manufacturer's instructions. First-strand cDNAs were synthesized using 1 µg of total RNA, oligo (dT) (Invitrogen, Carlsbad, CA, USA), and Superscript III reverse transcriptase (Invitrogen). Genes encoding murine *Ifna*, *Ifnb*, *Ifng*, *Il6*, *Tnfa*, *Stat1*, and *Actb* were amplified in a Real-time PCR Detection System (BIO-RAD, Tokyo, Japan). The primer sequences and numbers of universal probes used in this study were as follows; *Ifna* (left: 5′-tcaagccatccttgtgctaa-3′, right: 5′-gtcttttgatgtgaagaggttcaa-3′, universal probe: #3), *Ifnb* (left: 5′-ctggcttccatcatgaacaa-3′, right: 5′-agagggctgtggtggagaa-3′, universal probe: #18), *Ifng* (left: 5′-atctggaggaactggcaaaa-3′, right: 5′-ttcaagacttcaaagagtctgagg-3′, universal probe: #21), *Il6* (left: 5′-gctaccaaactggatataatcagga-3′, right: 5′-ccaggtagctatggtactccagaa-3′, universal probe: #6), *Tnfa* (left: 5′-tcttctcattcctgcttgtgg-3′, right: 5′-ggtctgggccatagaactga-3′, universal probe: #49), *Stat1* (left: 5′-tgagatgtcccggatagtgg-3′, right: 5′-cgccagagagaaattcgtgt-3′, universal probe: #99), and Actb (left: 5′-aaggccaaccgtgaaaagat-3′, right: 5′-gtggtacgaccagaggcatac-3′, universal probe: #56). Sample signals were normalized to the reference gene beta-actin using the ΔΔCt method: $\Delta Ct = \Delta Ct_{sample} - \Delta Ct_{reference}$, as described previously [32]. The percentages were then calculated for each sample relative to the control sample.

ELISA

We determined the IL-6 and TNF-α levels in serum obtained from wild-type and STAT1 KO mice 7 days after DSS challenge using OptEIA™ Mouse IL-6 and TNF-α ELISA Kits (BD Biosciences), according to the manufacturer's instructions.

Flow cytometry

The surface expression of CD11b and Ly6c was evaluated by flow cytometry on a FACSCanto II™ (BD Biosciences), and the results were analyzed with FlowJo software (Tree Star, Ashland, OR, USA), as described previously [33]. The maximum percentage of Ly6c-expressing $CD11b^+$ cells was calculated for each sample. A FACSAriaII™ (BD Biosciences) was used for the isolation of Ly6c-expressing $CD11b^+$ cells from the colon tissue of wild-type or STAT1 KO mice. The purity of the isolated cells was more than 95%.

Immunohistochemistry

Colon tissues obtained from mice at day 7 were fixed in 4% paraformaldehyde phosphate buffer solution, embedded in paraffin, then immunohistochemistry was performed as described previously [32, 34, 35]. After deparaffinization, antigen retrieval for phospho-STAT1 was performed with a reagent kit (pH 9.0) (415211, Nichirei Bioscience, Inc., Tokyo, Japan) at 95 °C for 20 min. Endogenous peroxidase activity was blocked by incubation with 0.3% hydrogen peroxide at room temperature for 10 min. After washing with rebuffed saline, sections were treated with anti-phospho-STAT1 (#9167, Cell Signaling Technology) antibodies overnight at 4 °C. Protein expression was visualized using N-Histofine Simple Stain MAX PO(R) (Nichirei Biosciences, Inc.). After washing, protein expression was visualized using 3-3′-diaminobezidine-4 HCl at room temperature for 5 min. Finally, all sections were counterstained with Mayer's hematoxylin. The formalin-fixed, paraffin-embedded sections were stained with HE.

Colon specimens from two patients with UC were formalin-fixed and paraffin-embedded and sections were stained with hematoxylin–eosin (HE). The slides were treated with anti-phospho-STAT1 (#9167, Cell Signaling Technology), anit-CD14 (MY4), anti-human CD68 (M0814, Dako ChemMate, Denmark A/S, Glostrup, Denmark), CD163 (NCL-CD163, Leica Biosystems, Newcastle, UK), and anti-CCR2 (clone; 7A7, ab6672, Abcam) antibodies. Protein expression was visualized using N-Histofine Simple Stain MAX PO (R) (Nichirei Biosciences, Inc.) and peroxidase (Envision/HRP; Dako, Tokyo, Japan). After washing, phosphor-STAT1, CD14, CD163, CD68, and CCR2 protein expression was visualized using 3-3′-diaminobezidine-4 HCL at room temperature for 5 min and 10 min. Finally, all sections were counterstained with Mayer's hematoxylin. Signal strength of CD14, CD163, CD68, and CCR2 in colon tissues of UC patients was calculated by ImageJ software.

Multicolor immunofluorescence staining

Triple-color immunofluorescence staining for the colon tissues of patients with UC was performed as described previously [36]. The sections were incubated with primary antibodies against CD68 (M0814, at 1:300 dilution, Dako ChemMate) and CCR2 (clone; 7A7, ab6672, Abcam) at 4 °C overnight. The samples were treated with secondary antibody, biotinylated anti-rabbit IgG, at room temperature for 30 min, and were then treated with AlexaFluor 488-conjugated streptavidin and AlexaFluor 594-conjugated anti-mouse IgG at room temperature for 30 min. Nuclei were counterstained with DAPI. The fluorescence signals were evaluated by confocal microscopy.

Statistical analysis

In vitro experiments were repeated between three and five times. In vivo experiments were independently performed two to four times. Mean values and SDs were calculated for each data set. Significant differences between groups were determined by a two-tailed Student's *t*-test. For some experiments, data were analyzed by one-way analysis of variance (ANOVA) and Dunnett's post-test. P values < 0.05 were considered statistically significant.

Results

Type I IFN–STAT1 signal cascade is augmented in the colon tissues of DSS-induced acute colitis model mice

To address the involvement of STAT1 activation in the steps of pathogenesis, including the onset, exacerbation, and subsequent chronicity of IBD, we established a DSS-induced acute colitis mouse model. Intake of DSS reduced the body weight of the mice, shortened the colon length, and the histology of the colon tissues showed disease states (Fig. 1A–C). In the acute colitis model mice, we found that the gene expression levels of IFN-α and IFN-β, but not IFN-γ, as well as IL-6 and TNF-α, were significantly upregulated in the colon tissues (Fig. 1D). Furthermore, we confirmed that the STAT1 gene expression level was augmented (Fig. 1E) in the inflamed colon tissues and phosphorylated STAT1 protein was detected in the pathological lesions (Fig. 1F). These findings suggested that Type I IFN (IFN-α/β)-mediated STAT1 activation may occur in the colon tissues during disease onset in acute colitis model mice.

STAT1 deficiency significantly reduces the pathogenesis of DSS-induced acute colitis in vivo

Next, we evaluated the effect of STAT1 in the pathogenesis of DSS-induced acute colitis using STAT1 KO mice. STAT1 deficiency significantly reduced the body weight loss of DSS-induced acute colitis model mice (Fig. 2A). Shortening of the colon length was significantly reduced in STAT1 KO mice compared with wild-type (WT) mice (Fig. 2B). Serum IL-6 and TNF-α levels were significantly decreased in STAT1 KO mice at day 7 (Fig. 2C). Histology of the colon tissues showed that inflammation in the lesions of WT mice was more severe than in STAT1 KO mice (Fig. 2D). The histological scores based on the severity of inflammation, the depth of injury, and crypt damage were significantly lower in the STAT1 KO mice (Fig. 2E).

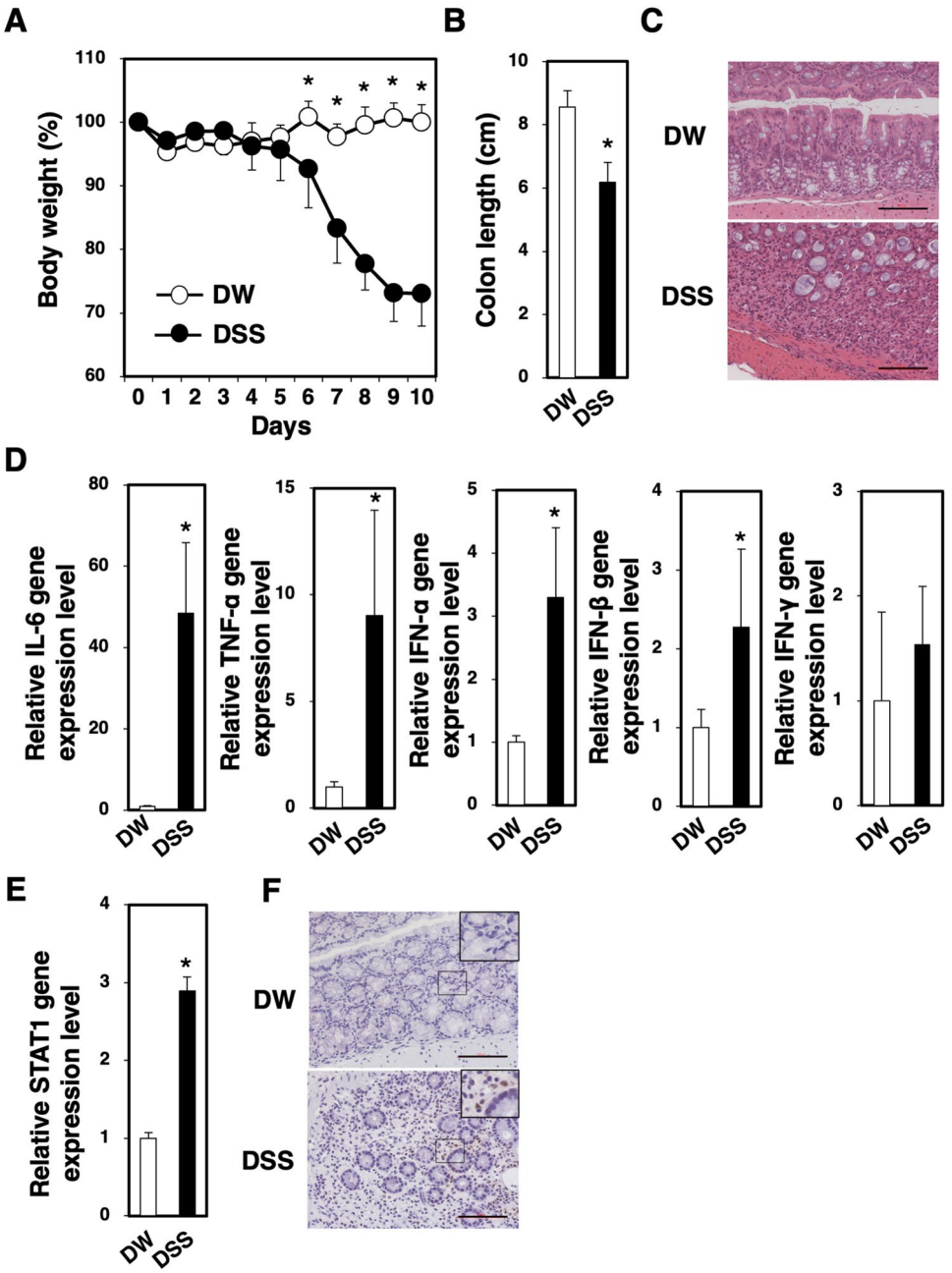

Fig. 1 Activation of STAT1 in the colon tissue of DSS-induced colitis mice. C57BL/6 wild type (WT) mice were administered 3% (w/v) DSS in drinking water for 7 days. On day 7, the DSS solution was replaced with normal drinking water. **A** Body weight of the control mice (DW, $n=6$) and DSS-treated mice (DSS, $n=6$) was monitored for 10 days and alterations in body weight compared with day 0 were calculated and are presented as percentages. $^*P<0.05$ by Student's *t*-test. The data are representative of four experiments of 4–8 mice per group. **B**, **C** Colons tissues were collected from the colitis model mice on day 7. HE staining was performed on sections of the lesions and inflammation areas. The data are representative of four experiments of 4–8 mice per group. Representative images are presented. Bars represent 200 μm. **D**, **E** IL-6, TNF-α, IFN-α, IFN-β, IFN-γ and STAT1 gene expression levels of whole cells collected from the colon tissues of DW- or DSS-treated mice were evaluated by quantitative PCR. The relative gene expression levels were calculated and the means and SDs of the two separate experiments performed in duplicate with six to eight colons per group are indicated in the figure. $^*P<0.05$ by Student's *t*-test. **F** Phosphorylated STAT1 protein was detected in the pathological lesions. Immunostaining using anti-phospho-STAT1 antibodies was performed on sections of colon tissue from DW-treated mice and the lesions and inflammation areas of DSS-treated mice. Representative images are presented. Bars represent 100 μm

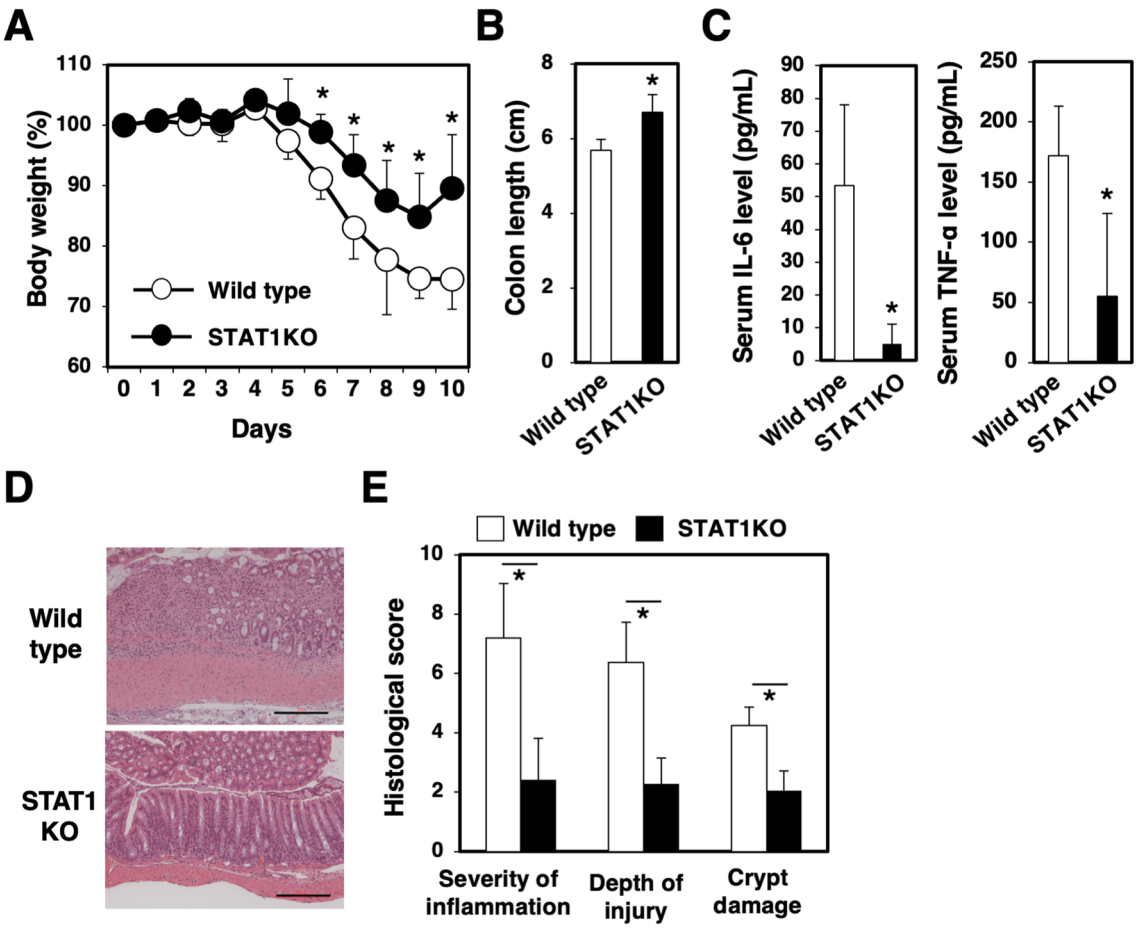

Fig. 2 Improvement of DSS-induced colitis under STAT1-deficient conditions. C57BL/6 wild type (WT) ($n=8$) and STAT1KO ($n=9$) mice were administered 3% DSS for 7 days. On day 7, the DSS solution was replaced with normal drinking water. **A**, **B** Body weight of the mice was monitored for 10 days and the Δbody weights (%) against day 0 were calculated. The data are representative of four experiments of 4–7 mice per group. **C** Serum IL-6 and TNF-α levels of DSS-treated WT and STAT1 KO mice were evaluated by ELISA. The data are representative of three experiments of 4–8 mice per group. Means and SDs ($n=6$) are indicated in the figure. $^*P<0.05$ by Student's *t*-test. **D**, **E** HE staining of colon tissues were performed on day 10 and histological score were evaluated. Representative images are presented. Bars represent 500 μm. Means and SDs are indicated in the figure. $^*P<0.05$ by Student's *t*-test

Transfer of bone marrow cells from WT mice augmented the reduction of body weight of DSS-treated STAT1 KO mice as well as WT mice on day 10, although the enhanced reduction of body weight was observed in the DSS-treated WT mice but not STAT1KO mice on day 6 (Fig. 3A). Transfer of bone marrow cells from WT mice augmented the shortening of the colon length of DSS-treated STAT1 KO mice that transferred with STAT1KO-derived bone marrow cells. The effect of WT bone marrow cells into STAT1 KO mice was similar to the case of the transfer into WT mice (Fig. 3B). Transfer of bone marrow cells from WT mice also exacerbated the histological scores based on the crypt damage, but not the severity of inflammation and depth of injury in the DSS-treated STAT1 KO mice, although all of the histological scores was exacerbated in the WT mice transferred with bone marrow cells from WT mice (Fig. 3C, D). These results suggested that STAT1 activation in hematopoietic cells may be associated with the pathogenesis of DSS-induced acute colitis.

Ly6c-highly expressing cells are induced in the inflamed colon tissues of DSS-induced acute colitis model mice in a STAT1-dependent manner

We investigated the immune cells that accumulated in the inflamed colon tissues of the DSS-induced acute colitis model mice. The ratios and numbers of total $CD45^+$ $7AAD^-$ cells of STAT1 KO mice were not altered in the colon tissues of WT mice (Fig. 4A). Moreover, the ratios

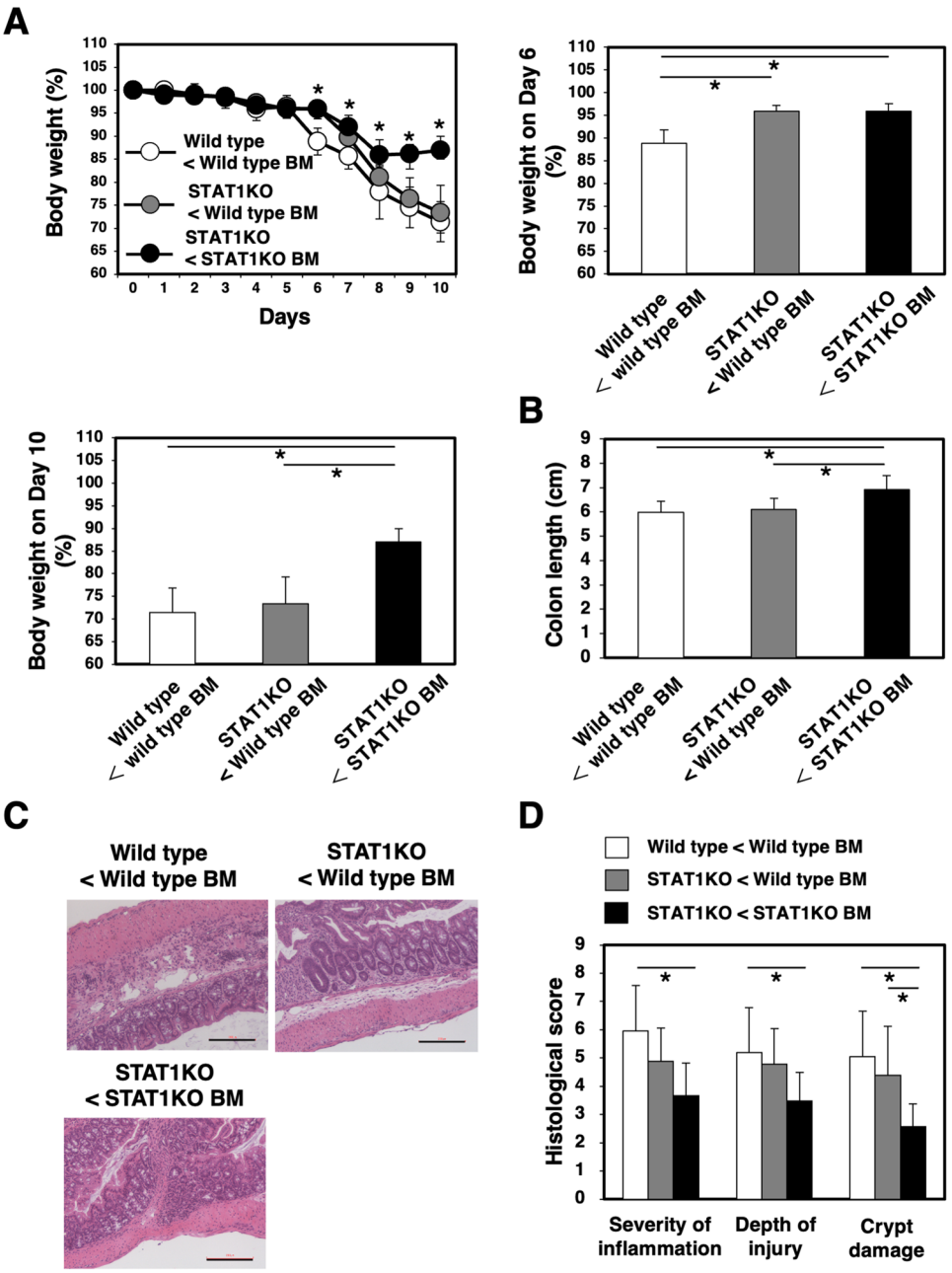

Fig. 3 Exacerbation of pathogenesis in DSS-induced colitis model with STAT1KO mice by transfer of bone marrow cells from WT mice. C57BL/6 wild type (WT) mice ($n=8$) were intravenously inoculated with bone-marrow cells (2×10^7) from WT mice and STAT1KO ($n=8, 9$) mice were inoculated with bone-marrow cells from WT or STAT1KO mice. The bone-marrow transferred WT and STAT1KO mice were administered 3% DSS for 7 days. On day 7, the DSS solution was replaced with normal drinking water. **A** Body weights of the WT and STAT1KO mice were monitored for 10 days and the Δbody weights (%) against day 0 were calculated. The representative data on day 6 and 10 are separately indicated in the figure. **B**, **C** Colons were collected from the mice on day 7 and the lengths and histological score were evaluated. Means and SDs are indicated in the figure. *$P<0.05$ by Student's *t*-test

of $CD4^+$ cells, $CD8^+$ cells, $CD11b^+$ cells, $CD11c^+$ cells, and Gr-1^+ cells among the $CD45^+$ $7AAD^-$ cells were not changed between WT and STAT1 KO mice, although the average of $CD8^+$ cells of WT mice were lower than STAT1 KO mice and $CD11b^+$ cells and $CD11c^+$ cells of WT mice were higher than STAT1 KO mice (Fig. 4B). In this study, we found that the accumulation of Ly6c-highly-expressing cells in the colon tissues was reduced in STAT1 KO mice (Fig. 4C, D). Furthermore, we confirmed that these cells expressed CD11b and partially CD11c on the cell surface (Supplementary Fig. S1). Flow cytometry using anti-Gr-1 antibody revealed that Ly6G/6C was intermediately expressed in the Ly6c-highly expressing cells. These data suggested that STAT1-mediated Ly6c-expressing cells may be involved in the inflammation and pathogenesis of acute colitis in vivo.

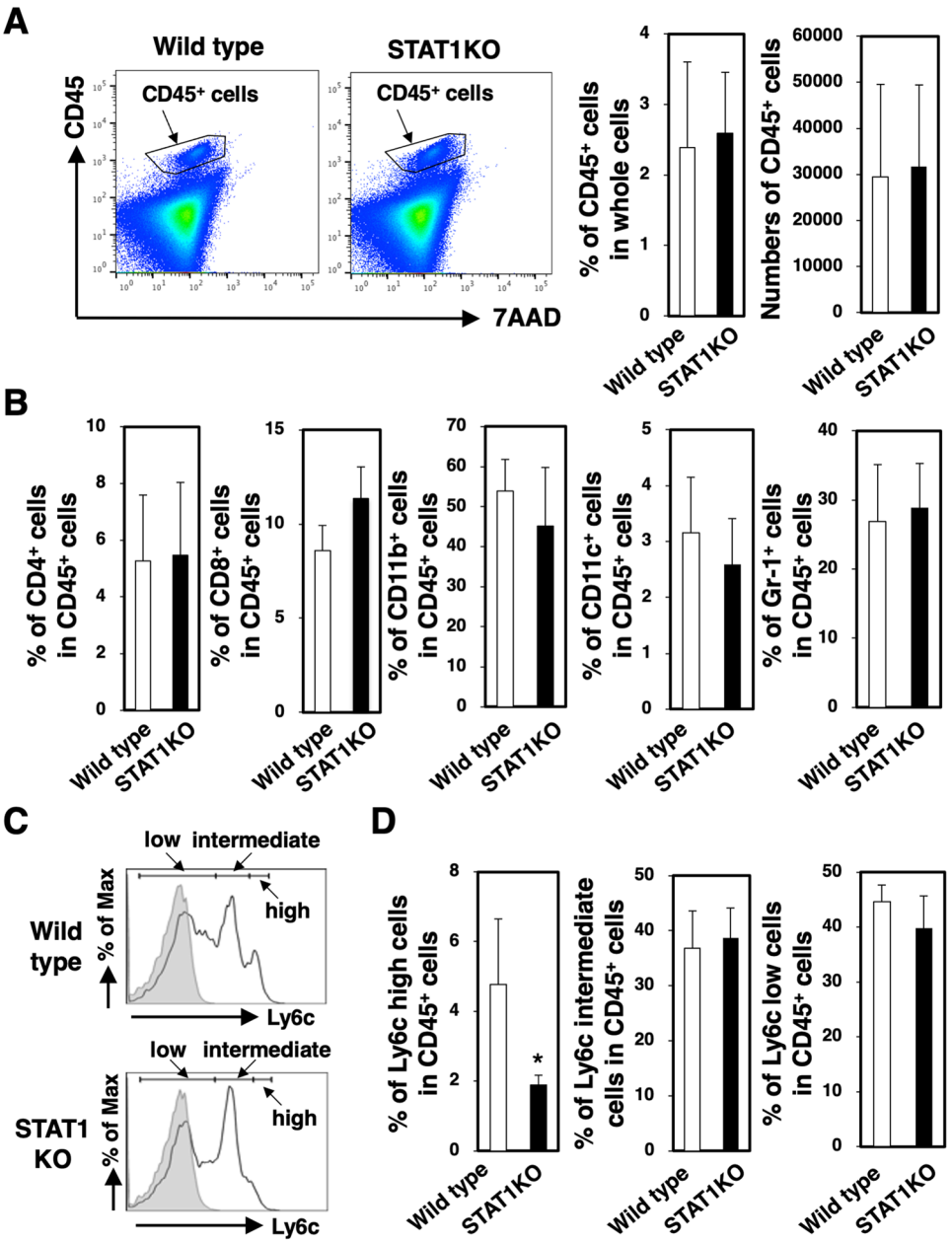

Fig. 4 Ly6c-highly expressing cell populations in the inflamed colon tissues of DSS-treated WT and STAT1 KO mice. C57BL/6 wild type (WT) and STAT1 KO mice were administered 3% DSS for 7 days. **A** Total cells were collected and pooled from the colon tissues of 3% DSS-induced colitis model mice at day 7. The percentages of 7AAD$^-$CD45$^+$ cells among the total cells were determined by flow cytometry. Representative profiles are indicated in the figure. The numbers of 7AAD$^-$CD45$^+$ cells were calculated from the numbers of the collected total colon cells. The data are pooled from four experiments of 4–6 mice per group. Means and SDs ($N=4$) are indicated. **B** The percentages of CD4$^+$, CD8$^+$, CD11b$^+$, or Gr-1$^+$ cells among CD45$^+$ cells were determined by flow cytometry. **C** Ly6c expression levels of 7AAD$^-$CD45$^+$ cells of the colon tissues of DSS-treated WT and STAT1 KO mice were evaluated by flow cytometry. Representative profiles are indicated in the figure. **D** Ratios of Ly6c-highly-expressing, intermediate-expressing, and low-expressing cells in the colon tissues of WT and STAT1 KO mice were calculated. Means and SDs ($N=4$) are indicated. *$P<0.05$ by Student's *t*-test

Ly6c-expressing cells are induced by stimulation with IFN-α/β in a STAT1-dependent manner

Next, we investigated the upstream effects of the STAT1-mediated induction of colitogenic effector cells in vitro. Ly6c-expressing cells were significantly induced by stimulation with IFN-α and IFN-β, and to a lesser extent IFN-γ, from both spleen cells and peritoneal exudate cells (PECs) in vitro (Fig. 5A, B, and Supplementary Fig. S2A, B). The IFN-α/β-induced Ly6c-highly expressing cells from spleen cells, but not PECs, partially expressed CD11b, CD11c, and MHC class II (Supplementary Fig. S3). A small portion of Ly6c-highly-expressing cells and intermediate-expressing cells were induced by STAT1-deficient spleen cells and PECs

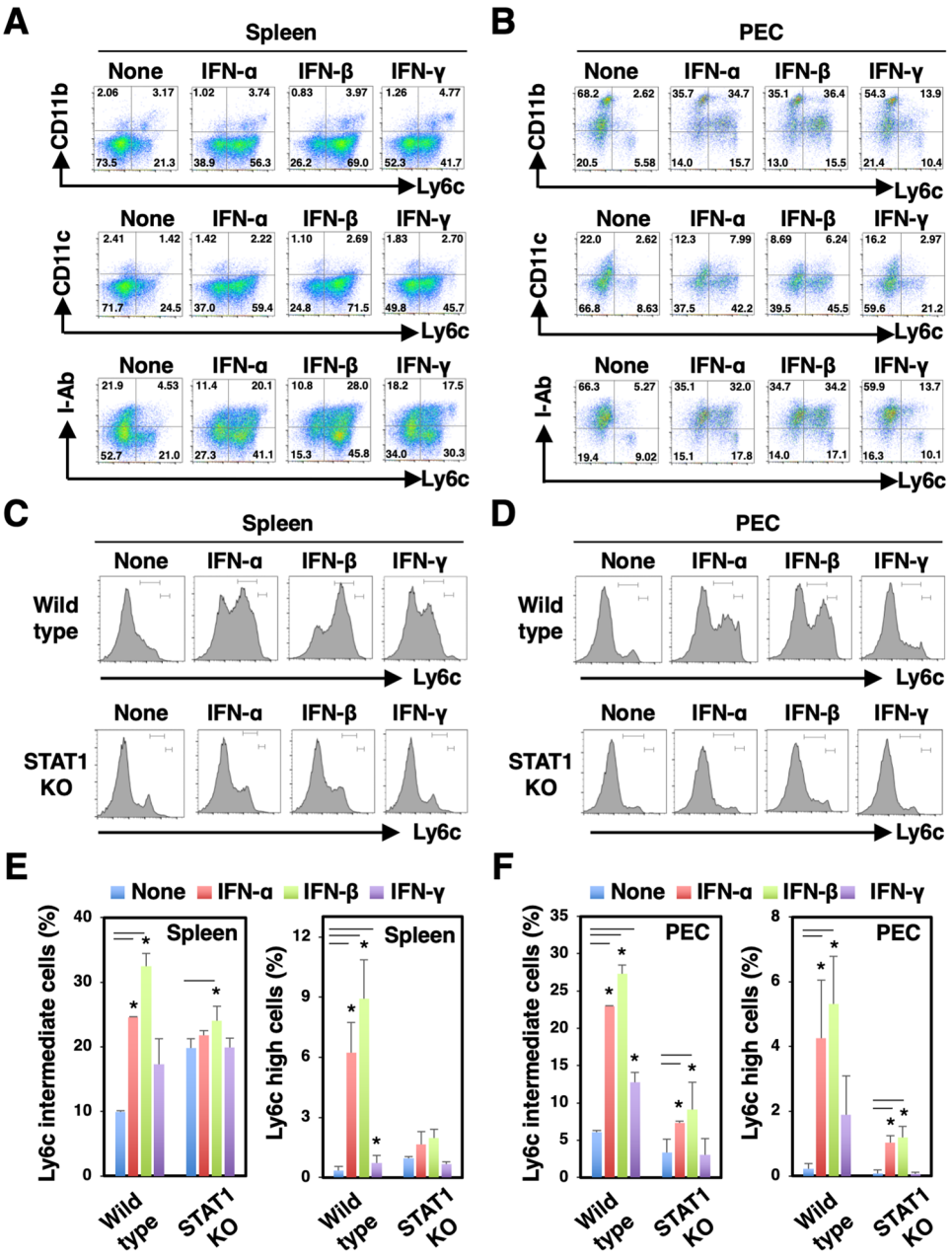

Fig. 5 IFNs induce Ly6c-expressing cells in a STAT1-dependent manner. Spleen cells and PECs were collected from C57BL/6 wild type (WT) mice and stimulated with IFN-α, IFN-β, or IFN-γ for 24 h in vitro. **A**, **B** CD11b, CD11c, and I-Ab expression levels of the Ly6c-expressing cells in IFN-treated spleen cells (**A**) and PECs (**B**) were evaluated by flow cytometry. Representative profiles and the percentage of cell numbers in each quadrant are indicated in the figure. **C**, **D** Ly6c expression levels of 7AAD$^-$CD45$^+$ cells of the IFN-treated spleen cells (**C**) and PECs (**D**) were evaluated by flow cytometry. Representative profiles are indicated in the figure. **E**, **F** Ratios of Ly6c-highly expressing and intermediate-expressing cells in the IFN-treated spleen cells (**E**) and PECs (**F**) of WT and STAT1 KO mice were calculated. Means and SDs are calculated from the data of four samples of each mouse and one representative result from three independent experiments is indicated in the figure. *$P < 0.05$ by Dunnett's test

(Fig. 5C–F). These data suggested that Type I IFNs, IFN-α/β may be preferentially involved in the induction of STAT1-mediated colitogenic Ly6c-expressing macrophages.

Ly6c-highly expressing macrophages induce the IL-6 and CCL2/CCR2 genes and Ly6c-intermediate-expressing macrophages induce the TNF-α and IFN-α/β genes in DSS-induced acute colitis

Next, we evaluated the gene expression levels of inflammation-related chemokines, chemokine receptors, and cytokines in Ly6c-expressing macrophages in the colon tissues of DSS-induced acute colitis model mice. Whole colon and spleen cells were collected from the inflamed colon tissues and spleen of WT mice, respectively. Ly6c$^+$ cells, Ly6c-high-expressing cells, and Ly6c-intermediate-expressing cells were isolated from CD45$^+$7AAD$^-$ cells of the whole colon cells. Ly6c$^+$ cells were isolated from CD45$^+$7AAD$^-$ cells in the inflamed colon tissues of WT mice. The gene expression levels of proinflammatory cytokines, chemokines, and chemokine receptors were evaluated by quantitative PCR. The gene expression levels of IL-6, CCR2, and CCL2 were higher in Ly6c-highly expressing macrophages compared with Ly6c-intermediate-expressing and low-expressing macrophages (Fig. 6A).

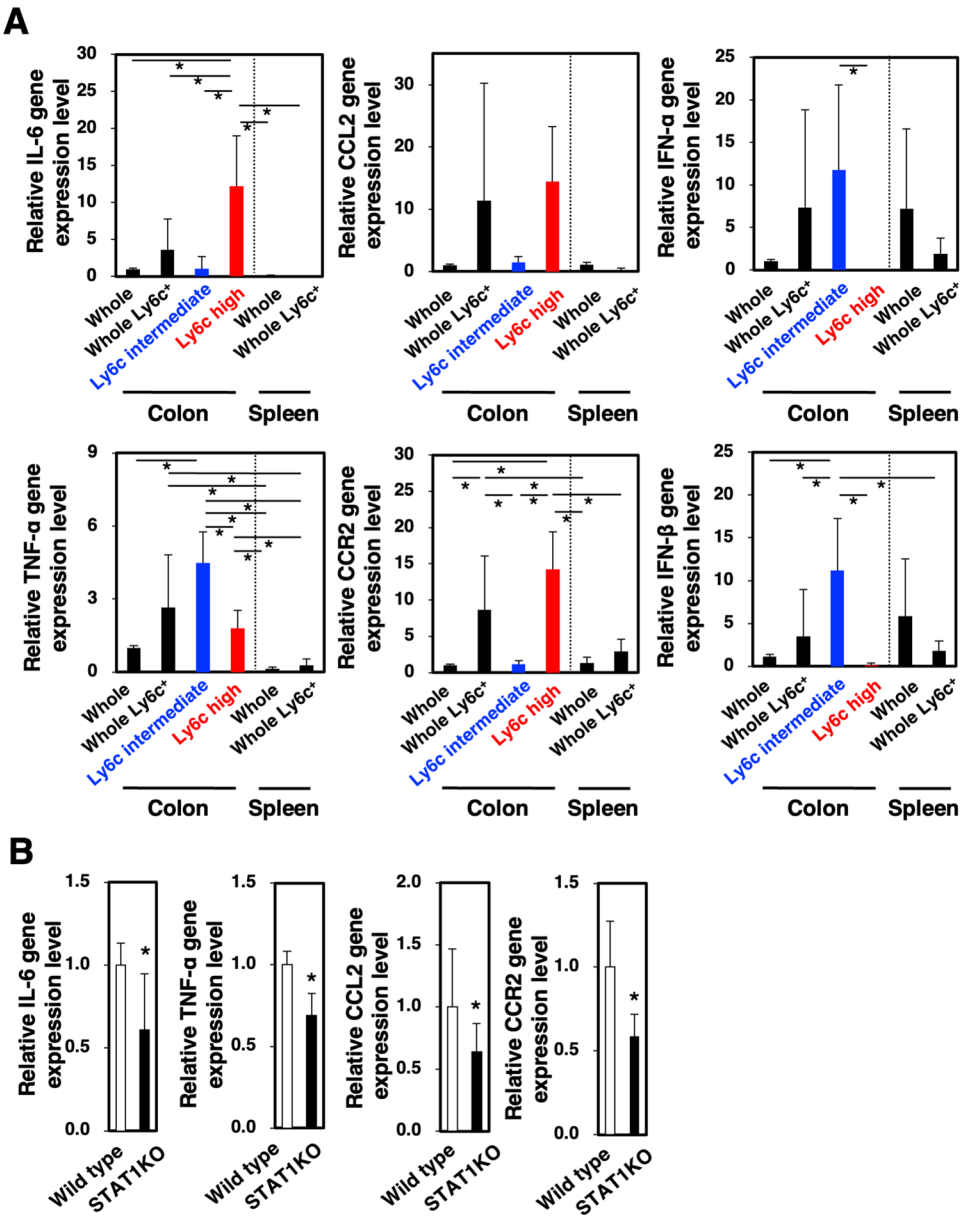

Fig. 6 CCL2 and CCR2 but not IFN-α/β gene expression levels in Ly6c-highly expressing cells in the inflamed colon of colitis mice were high compared with Ly6c-intermediate-expressing cells. Whole cells and whole Ly6c$^+$ cells were collected from colon and spleen of DSS-treated C57BL/6 wild type (WT) mice. The data are pooled from four experiments of 13–21 mice per group. CD45$^+$7AAD$^-$Ly6c-highly expressing and Ly6c-intermediate-expressing cells were collected from the pooled colon tissues of DSS-treated WT mice. **A** Gene expression levels of IL-6, TNF-α, CCL2, CCR2, IFN-α, and IFN-β for each cell were evaluated by quantitative PCR. Quantitative PCR was carried out in duplicate for each sample from two independent experiments. The relative gene expression levels were calculated and the means and SDs ($N=4$) are indicated in the figure. *$P<0.05$ by Dunnett's test. **B** Gene expression levels of IL-6, TNF-α, CCL2, and CCR2 of whole cells collected from DSS-treated WT and STAT1 KO mice were evaluated by quantitative PCR. The relative gene expression levels were calculated and the means and SDs ($N=4$) are indicated in the figure. *$P<0.05$ by Student's *t*-test

The gene expression levels of TNF-α and IFN-α/β were higher in Ly6c-intermediate-expressing and low-expressing macrophages compared with Ly6c-highly expressing cells (Fig. 6A). We further confirmed that the IL-6, TNF-α, CCR2, and CCL2 gene expression levels in all of the Ly6c-expressing cells from colon tissues of the acute colitis model mice were higher than those of cells from the spleen of acute colitis model mice (Fig. 6A). The gene expression levels of IL-6, TNF-α, CCL2, and CCR2 were significantly reduced in the inflamed colon tissues from STAT1 KO mice compared with WT mice (Fig. 6B).

These data suggested that Ly6c-expressing macrophages may differentiate into inflammatory pathogenic effector cells during the process of colitis in a STAT1-dependent manner in vivo.

Blockade of CCR2-mediated signaling significantly reduces the pathogenesis of DSS-induced acute colitis

We tried to identify the involvement of CCR2-mediated signaling in the pathogenesis of DSS-induced acute colitis. In vivo injection of the CCR2 antagonist into wild type mice significantly reduced the body weight loss of DSS-induced acute colitis mice, whereas STAT1KO mice administrated with the CCR2 antagonist did not show the improvement of bodyweight loss (Fig. 7A). Shortening of the colon length was significantly reduced in the CCR2 antagonist-treated wild type but not STAT1KO mice compared with the control mice (Fig. 7B). Serum IL-6 and TNF-α levels were significantly decreased in the CCR2 antagonist-treated wild type

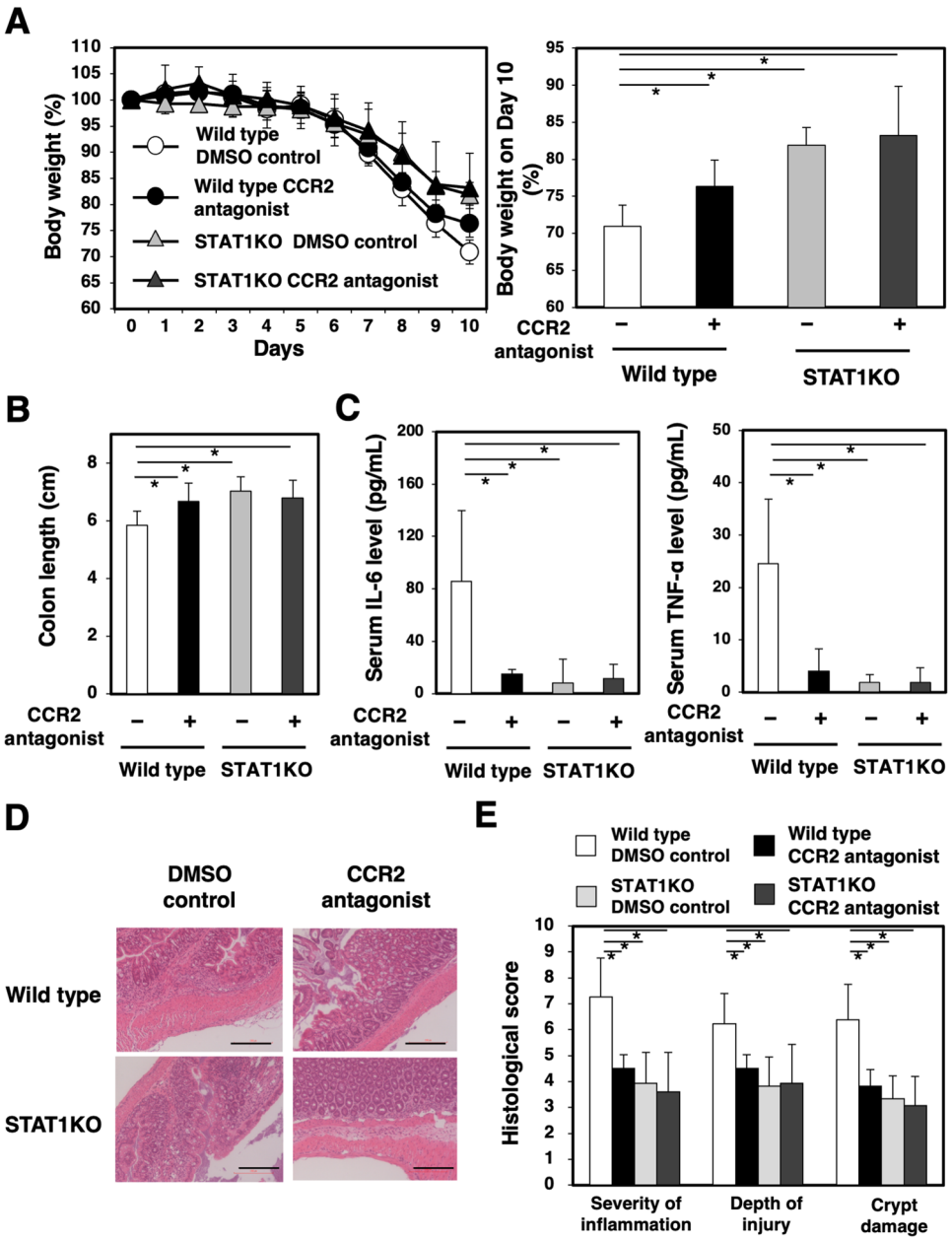

Fig. 7 In vivo administration of a CCR2 antagonist improved the disease state of DSS-induced acute colitis modes. C57BL/6 wild type (WT) and STAT1KO mice were administered 3% (w/v) DSS in drinking water (DW) for 7 days. On day 7, the DSS solution was replaced with normal drinking water. DMSO, as a control, or CCR2 antagonist (20 μg in 200 μL of PBS) was intraperitoneally injected into the DSS-treated or DW control mice every day from day −1. **A**, **B** Body weights of the DMSO control mice and CCR2 antagonist-treated mice were monitored for 10 days and alterations in body weights as a percentage of that at day 0 are presented. Colons were collected from the mice on day 7 and the colon lengths at day 7 are indicated in the figure. The data are representative of three experiments of 4–8 mice per group. **C** Serum IL-6 and TNF-α levels of the DMSO control- and CCR2 antagonist-treated mice were evaluated by ELISA. The data are representative of two experiments of 5–8 mice per group and the means and SDs (DMSO control $n=7$, CCR2 antagonist $n=8$) are indicated in the figure. **D** HE staining of colon tissues were performed on day 7. Representative images are presented. Bars represent 200 μm. **E** Histological scores of colitis induced by 3% DSS administration were evaluated at day 7. Means and SDs (DMSO control $n=8$, CCR2 antagonist $n=8$) of the severity of inflammation, the depth of injury, crypt damage, and the total score are indicated in the figure

mice at day 7, although the inflammatory cytokine levels were low and not altered between the CCR2 antagonist-treated and the control STAT1KO mice (Fig. 7C). The histology of the colon tissues of wild type mice showed that inflammation in the lesions of the control mice was more severe than in the CCR2 antagonist-treated wild type mice

and the severity of CCR2 antagonist-treated STAT1KO mice was similar with those of the CCR2 antagonist-treated wild type mice and the control STAT1KO mice (Fig. 7D). Disease indicators such as the severity of inflammation, the depth of injury, and crypt damage were significantly lower in the CCR2 antagonist-treated wild type mice (Fig. 7E). The scores of CCR2 antagonist-treated STAT1KO mice was similar with those of the CCR2 antagonist-treated wild type mice and the control STAT1KO mice. These data suggested that CCR2-mediated signaling is involved in the inflammation and pathogenesis of DSS-induced acute colitis in a STAT1-dependent manner.

CCR2-expressing macrophages accumulate in the inflamed colon tissues of UC patients

Finally, we investigated the activation of STAT1 and CCR2 expression in the lesions of patients with UC. Phosphorylated STAT1 and CCR2 were expressed in the inflamed colon tissue and infiltration of CD14-, CD68-, and CD163-expressing monocytes and macrophages was observed in the lesions of UC patients (Fig. 8A). In this study, we found that CCR2 was expressed in some of the CD68-positive macrophages in the inflamed colon tissues (Fig. 8B). Furthermore, we confirmed that Pt#1 (Active UC, Severe, Matts grade 4) showed low expression levels of CD14 and high expression levels of CD163, and CCR2 but not CD68 compared to Pt#2 (Active UC, Moderate, Matts grade 3) (Fig. 8C), suggesting that the severity of pathogenesis might be related to the expression levels of CD163 and CCR2. Based on these data we speculate that STAT1 and CCR2-mediated signal cascades may be involved in the induction of colitogenic inflammatory macrophages and the onset, exacerbation, and subsequent chronicity of human IBD.

Discussion

In this study, we showed that the infiltration of Ly6c-highly-expressing cells into the colorectal tissues of acute colitis model mice was attenuated in STAT1 KO mice. The gene expression levels of IL-6, CCL2, and CCR2 in Ly6c-highly

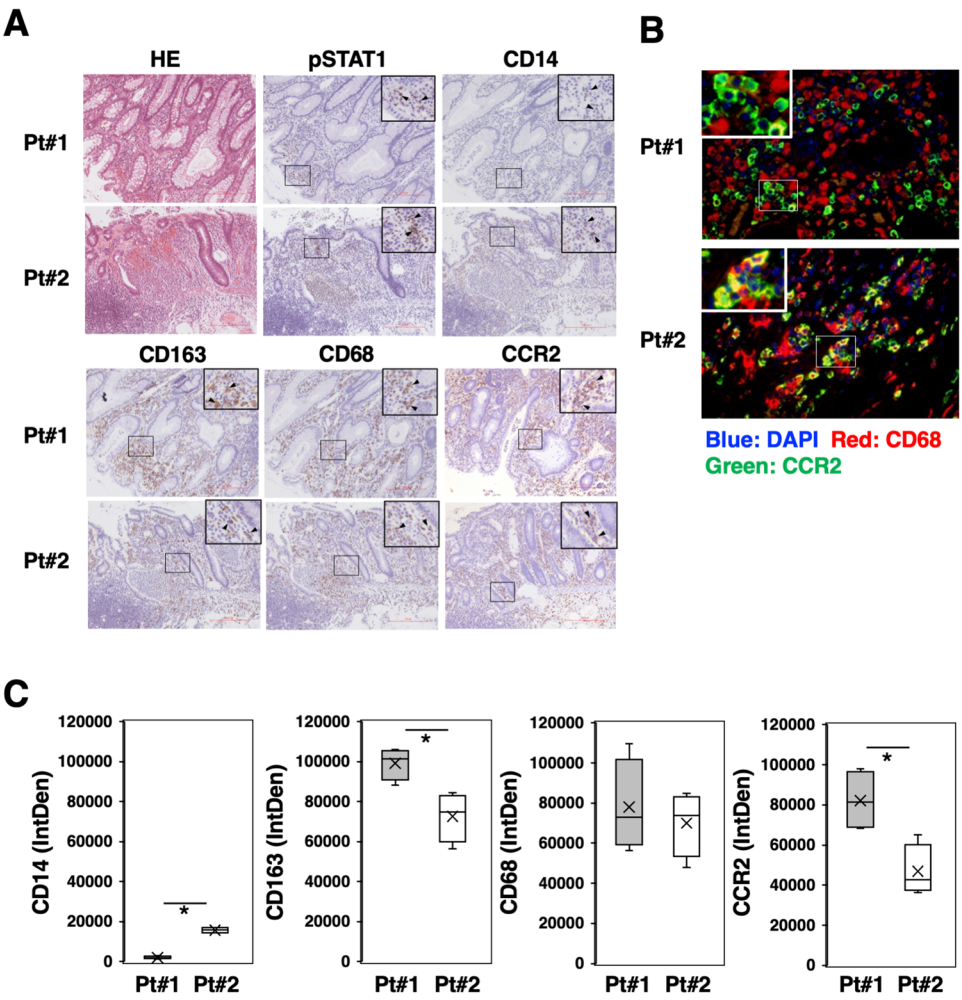

Fig. 8 Activation of STAT1 and expression of CCR2 in $CD68^+$ macrophages in the lesion of a patient with UC. **A** Hematoxylin and eosin (HE) staining and immunostaining using anti-pSTAT1, anti-CD14, anti-CD168, anti-CD68, anti-CD68, or anti-CCR2 antibodies were performed for sections of the lesions and inflammation areas from two representative patients with ulcerative colitis (UC). Representative microphotographs are indicated. Bars indicate 200 µm. **B** Triple-immunofluorescence staining of CD68 (red) and phosphor-STAT1 or CCR2 (green) was performed for the sections from two patients with UC. Blue indicates cell nuclei stained with DAPI. **C** Signal strengths of CD14, CD163, CD68, and CCR2 in colon tissues of UC patients were calculated by ImageJ software. Box plots of the data are shown

expressing cells accumulated in the inflamed colon tissues of WT mice and were significantly higher than in Ly6c-intermediate-expressing cells, whereas TNF-α and IFN-α/β gene expression was higher in Ly6c-intermediate-expressing cells. Moreover, we confirmed that IFN-α/β rather than IFN-γ induced Ly6c-expressing cells from the spleen or PECs in a STAT1-dependent manner in vitro. These findings suggest that the two different types of Ly6c-expressing macrophages, preferentially induced by IFN-α/β, and may collaborate like as an IFN-α/β producer and a recruiter or conductor of colitogenic effectors and involved in the pathogenesis of the DSS-induced colitis model.

Generally, exogenous virus and bacterium infections induced type I IFNs in vivo [37]. Phylotype-level 16S rRNA analysis revealed that the bacterial families, Ruminococcaceae, Bacteroidaceae, Enterobacteriaceae, Deferribacteraceae, and Verrucomicrobiaceae increased in relative abundance in DSS-treated mice [22]. Therefore, we speculated that the type I IFN-mediated STAT1 activation by gut microbiota was closely related to the subsequent pathogenesis of acute colitis. Previous studies demonstrated the crucial roles of STAT1-mediated induction of Ly6c-expressing macrophages in the pathogenesis and onset of parasite infection in models with *Leishmania* and *Toxoplasma* [38–40]. Furthermore, there are several reports about the immunosuppressive or stimulatory roles of Ly6c-expressing macrophages in various cancers including colorectal cancers [41–44]. Therefore, it is important to understand the diversity and heterogeneity of Ly6c-expressing macrophages and to elucidate the regulatory mechanisms in the development of inflammation, which may lead to new prevention and therapeutic strategies for IBDs, as well as other infectious diseases and cancer.

A previous study revealed the increased expression and activation of STAT1 in biopsies of the inflamed mucosa of UC and CD patients compared with the normal mucosa [28]. The expression and activation of STAT1 are predominantly heightened in the inflamed mucosa of UC patients, and phosphorylated STAT1 was detected in monocytic cells and neutrophils in the inflamed mucosa. Another study indicated that Type I IFN, IFN-β, was produced in the intestinal tissues of IBD patients and activated T cells to induce colitogenic effector cells [15]. These findings strongly suggest that Type I IFN-mediated STAT1 activation in macrophages is associated with the onset and development of IBD.

A previous study demonstrated that CCR2 expression was essential to the recruitment of Ly6c-highly expressing monocytes to the inflamed gut to become the dominant mononuclear cell type in the lamina propria during acute colitis and the ablation of Ly6c-highly expressing monocytes ameliorated acute gut inflammation [45]. It was also reported that blockade of chemokine receptors CCR2, CCR5, and CXCR3 by antagonists, protected mice from DSS-induced colitis model [46]. Recent studies demonstrated that CCL2 production by macrophages was closely related to the onset of colitis [47–49]. In this study, we showed a decrease in Ly6c-highly expressing cells in the inflamed colon tissues of STAT1 KO mice compared with WT mice. In addition, we found that the gene expression levels of IL-6, CCR2, and CCL2 were higher in Ly6c-highly expressing cells. We confirmed that stimulation with Type-I IFNs induced Ly6c-expressing cells from the PECs and spleen cells of wild-type mice. The induction of Ly6c-expressing cells was significantly reduced or not induced at all in STAT1 KO mice. On the basis of these findings, we speculated that Type I IFN–STAT1 signaling in myeloid precursor cells is required for the induction of two different types of Ly6c-expressing macrophages, suggesting that the amelioration of acute colitis in STAT1 KO mice was caused by the inhibition of recruitment of the colitogenic macrophages into the inflamed colon tissues in a CCL2/CCR2-dependent manner.

Once the newly extravagated monocytes are stimulated by microorganisms and the cytokines from resident immune cells or epithelial cells, they transform into inflammatory M1-type macrophages to promote colonic inflammation via the production of pro-inflammatory cytokines, such as IL-6 and TNF-α. It is reported that autonomous TNF is critical for in vivo monocyte survival, maintenance, and function in a steady state and during inflammation [50]. It is also reported that human $CCR2^{+}$ monocytes release TNF by stimulation [51]. On the basis of these findings, we speculate that Ly6c-highly expressing macrophages produce TNF, function in inflamed colon tissues, and may be related to the pathology of our DSS-induced acute colitis model.

Drug therapy for IBD includes aminosalicylates, corticosteroids, immunosuppressive drugs, and biologic drugs, although these are unable to cure all patients [52]. During the pathogenesis of IBD, innate immune cells such as macrophages and dendritic cells directly drive intestinal inflammation by releasing large amounts of inflammatory cytokines, such as tumor necrosis factor TNF-α, IL-6, IL-12, or IL-23 [13–18]. Recently, several clinical studies were conducted to evaluate the efficacy of antagonists against the p19 subunit of IL-23 or the p40 subunit of IL-12 and IL-23 for IBD patients [53–55]. One biologic drug, antagonizing anti-TNF-α monoclonal antibody, is effective but the loss of response to infliximab was observed in 37% of CD patients [56–60]. Severe UC is one of the risk factors for colorectal cancer, resulting in the appearance of cancer cells and the promotion tumorigenesis leading to colorectal cancer. Therefore, novel approaches are needed to maintain complete remission of IBD. Our experimental models reveal that the Type-I IFN/STAT1–CCL2/CCR2 axis in macrophages is associated with acute colitis. Furthermore, we confirmed activation of STAT1 and infiltration of CCR2-expressing macrophages into the lesions and inflammation sites of

colorectal tissues in UC and CD patients, suggesting a promising target to prevent the initial steps of pathogenesis through from onset, to exacerbation, and the subsequent chronicity of IBDs.

In conclusion, the IFN-α/β-mediated activation of STAT1 in myeloid precursor cells and two different types of Ly6c-expressing cells induced in inflamed colon tissues are associated with the initial steps of pathogenesis of colitis. Interactions with Ly6C-high-expressing and intermediate-expressing macrophage subsets may play an important role in the onset and progression of IBD. From these results, we speculated that blockade of the Type I IFN–STAT1 signaling cascade might be a new therapeutic option to prevent and/or ameliorate the initial onset of IBD.

Supplementary Information The online version contains supplementary material available at https://doi.org/10.1007/s00011-022-01620-z.

Acknowledgements We thank Dr. Y. Ohno, Dr. N. Okada, and Dr. K. Sugiyama for their excellent and thoughtful advice on this study. This work was partially supported by a Grants-in-Aid for Scientific Research (C) (15K08416 to H.K.) and by a Grants-in-Aid for Scientific Research (B) (16H05409 to A.T.) from the Japan Society for the Promotion of Science (JSPS), the Platform Project for Supporting Drug Discovery and Life Science Research (Platform for Drug Discovery, Informatics, and Structural Life Science) from the Ministry of Education, Culture, Sports, Science and Technology (MEXT) of Japan (H.K.), the Japan Agency for Medical Research and Development (AMED) (H.K. and A.T.), and the Joint Research Program of the Institute for Genetic Medicine, Hokkaido University (S.H., M.T., and A.T.). We thank Kate Fox, DPhil, from Edanz Group (https://en-author-services.edanzgroup.com/ac) for editing a draft of this manuscript.

Author contributions H.K. and A.T. conceived the project. H.K. designed the experiments. S.K. performed experiments and wrote the manuscript. S.K., S.H., K.I., M.T., and H.K. analyzed and interpreted the results. N.I., T.Y., S.H., and A.T. provided clinical samples and advice. M.T. and S.K. performed the histological analyses. A.T. generated and evaluated clinical data and guided the work.

Declarations

Conflict of interest The authors have no conflicts of interest to disclose.

Ethics approval statement for human and animal studies Research protocols involving human subjects were approved by the institutional review board of Hokkaido University Graduate School of Medicine (14-043) and the Institute for Genetic Medicine (14-0004). Written informed consent was obtained from all patients. All procedures in this study were carried out in accordance with the relevant guidelines and regulations and according to the Declaration of Helsinki. All mouse experiments were approved by the Animal Ethics Committee of Hokkaido University (No. 14-0039, 19-0035, 19-0065) and were conducted in accordance with the recommendations in the Guide for the Care and Use of Laboratory Animals of the University.

References

1. Ng SC, Shi HY, Hamidi N, Underwood FE, Tang W, et al. Worldwide incidence and prevalence of inflammatory bowel disease in the 21st century: a systematic review of population-based studies. Lancet. 2017;390(10114):2769–78.
2. Kaplan GG. The global burden of IBD: from 2015 to 2025. Nat Rev Gastroenterol Hepatol. 2015;12(12):720–7.
3. Plichta DR, Graham DB, Subramanian S, Xavier RJ. Therapeutic opportunities in inflammatory bowel disease: mechanistic dissection of host-microbiome relationships. Cell. 2019;178(5):1041–56.
4. Ananthakrishnan AN, Bernstein CN, Iliopoulos D, Macpherson A, Neurath MF, Ali RAR, et al. Environmental triggers in IBD: a review of progress and evidence. Nat Rev Gastroenterol Hepatol. 2018;15(1):39–49.
5. Al Nabhani Z, Dulauroy S, Marques R, Cousu C, Al Bounny S, Déjardin F, et al. A weaning reaction to microbiota is required for resistance to immunopathologies in the adult. Immunity. 2019;50(5):1276–88.
6. Borbet TC, Blaser MJ. Host genotype and early life microbiota alterations have additive effects on disease susceptibility. Mucosal Immunol. 2019;12(3):586–8.
7. Fachi JL, Felipe JS, Pral LP, da Silva BK, Corrêa RO, de Andrade MCP, et al. Butyrate protects mice from *Clostridium difficile*-induced colitis through an HIF-1-dependent mechanism. Cell Rep. 2019;27(3):750–61.
8. Rangan P, Choi I, Wei M, Navarrete G, Guen E, Brandhorst S, et al. Fasting-mimicking diet modulates microbiota and promotes intestinal regeneration to reduce inflammatory bowel disease pathology. Nat Rev Gastroenterol Hepatol. 2019;26(10):2704–19.
9. Schirmer M, Garner A, Vlamakis H, Xavier RJ, et al. Microbial genes and pathways in inflammatory bowel disease. Nat Rev Microbiol. 2019;17(8):497–511.
10. Zuo T, Lu XJ, Zhang Y, Cheung CP, Lam S, Zhang F, et al. Gut mucosal virome alterations in ulcerative colitis. Gut. 2019;68(7):1169–79.
11. Norman JM, Handley SA, Baldridge MT, Droit L, Liu CY, Keller BC, et al. Disease-specific alterations in the enteric virome in inflammatory bowel disease. Cell. 2015;160(3):447–60.
12. Ungaro F, Massimino L, D'Alessio S, Danese S. The gut virome in inflammatory bowel disease pathogenesis: from metagenomics to novel therapeutic approaches. United Eur Gastroenterol J. 2019;7(8):999–1007. https://doi.org/10.1177/2050640619876787.
13. Bain CC, Scott CL, Uronen-Hansson H, Gudjonsson S, Jansson O, Grip O, et al. Resident and pro-inflammatory macrophages in the colon represent alternative context-dependent fates of the same Ly6Chi monocyte precursors. Mucosal Immunol. 2013;6(3):498–510.
14. Nakanishi Y, Sato T, Ohteki T, et al. Commensal gram-positive bacteria initiates colitis by inducing monocyte/macrophage mobilization. Nat Rev Gastroenterol Mucosal Immunol. 2015;8(1):152–60.
15. Giles EM, Sanders TJ, McCarthy NE, Lung J, Pathak M, MacDonald TT, et al. Regulation of human intestinal T-cell responses by type 1 interferon-STAT1 signaling is disrupted in inflammatory bowel disease. Mucosal Immunol. 2017;10(1):184–93.
16. Bernardo D, Marin AC, Fernández-Tomé S, Montalban-Arques A, Carrasco A, Tristán E, et al. Human intestinal pro-inflammatory CD11chighCCR2+CX3CR1+ macrophages, but not their tolerogenic CD11c-CCR2-CX3CR1- counterparts, are

expanded in inflammatory bowel disease. Mucosal Immunol. 2018;11(4):1114–26.
17. Na YR, Stakenborg M, Seok SH, Matteoli G, et al. Macrophages in intestinal inflammation and resolution: a potential therapeutic target in IBD. Nat Rev Gastroenterol Hepatol. 2019;16(9):531–43.
18. Eftychi C, Schwarzer R, Vlantis K, Wachsmuth L, Basic M, Wagle P, et al. Temporally distinct functions of the cytokines IL-12 and IL-23 drive chronic colon inflammation in response to intestinal barrier impairment. Immunity. 2019;51(2):367–80.
19. Rauch I, Müller M, Decker T. The regulation of inflammation by interferons and their STATs. JAK-STAT. 2013;2(1):e23820.
20. Decker T, Stockinger S, Karaghiosoff M, Müller M, Kovarik P. IFNs and STATs in innate immunity to microorganisms. J Clin Investig. 2002;109(10):1271–7.
21. Ivashkiv LB. IFNγ: signalling, epigenetics and roles in immunity, metabolism, disease and cancer immunotherapy. Nat Rev Immunol. 2018;18(9):545–58.
22. Berry D, Schwab C, Milinovich G, Reichert J, Ben Mahfoudh K, Decker T, et al. Phylotype-level 16S rRNA analysis reveals new bacterial indicators of health state in acute murine colitis. ISME J. 2012;6(11):2091–106.
23. Crnčec I, Modak M, Gordziel C, Svinka J, Scharf I, Moritsch S, et al. STAT1 is a sex-specific tumor suppressor in colitis-associated colorectal cancer. Mol Oncol. 2018;12(4):514–28.
24. Kang YH, Biswasx A, Field M, Snapper SB. STAT1 signaling shields T cells from NK cell-mediated cytotoxicity. Nat Commun. 2019;10(1):912.
25. Nakanishi Y, Sato T, Takahashi K, Ohteki T, et al. IFN-γ-dependent epigenetic regulation instructs colitogenic monocyte/macrophage lineage differentiation in vivo. Mucosal Immunol. 2018;11(3):871–80.
26. Wu X, Guo W, Wu L, Gu Y, Gu L, Xu S, et al. Selective sequestration of STAT1 in the cytoplasm via phosphorylated SHP-2 ameliorates murine experimental colitis. J Immunol. 2012;189(7):3497–507.
27. Bandyopadhyay SK, de la Motte CA, Kessler SP, Hascall VC, Hill DR, Strong SA, et al. Hyaluronan-mediated leukocyte adhesion and dextran sulfate sodium-induced colitis are attenuated in the absence of signal transducer and activator of transcription 1. Am J Pathol. 2008;173(5):1361–8.
28. Schreiber S, Rosenstiel P, Hampe J, Nikolaus S, Groessner B, Schottelius A, et al. Activation of signal transducer and activator of transcription (STAT) 1 in human chronic inflammatory bowel disease. Gut. 2002;51(3):379–85.
29. Kitamura H, et al. IL-6-STAT3 controls intracellular MHC class II alphabeta dimer level through cathepsin S activity in dendritic cells. Immunity. 2005;23(5):491–502.
30. Okayasu I, Hatakeyama S, Yamada M, Ohkusa T, Inagaki Y, Nakaya R. A novel method in the induction of reliable experimental acute and chronic ulcerative colitis in mice. Gastroenterology. 1990;98(3):694–702.
31. Dieleman LA, Palmen MJ, Akol H, Bloemena E, Peña AS, Meuwissen SG, et al. Chronic experimental colitis induced by dextran sulphate sodium (DSS) is characterized by Th1 and Th2 cytokines. Clin Exp Immunol. 1998;114(3):385–91.
32. Ohno Y, Kitamura H, Takahashi N, Ohtake J, Kaneumi S, Sumida K, et al. IL-6 down-regulates HLA class II expression and IL-12 production of human dendritic cells to impair activation of antigen-specific CD4(+) T cells. Cancer Immunol Immunother. 2016;65(2):193–204.
33. Ohno Y, Toyoshima Y, Yurino H, Monma N, Xiang H, Sumida K, et al. Lack of interleukin-6 in the tumor microenvironment augments type-1 immunity and increases the efficacy of cancer immunotherapy. Cancer Sci. 2017;108(10):1959–66.
34. Kitamura H, Ohno Y, Toyoshima Y, Ohtake J, Homma S, Kawamura H, et al. Interleukin-6/STAT3 signaling as a promising target to improve the efficacy of cancer immunotherapy. Cancer Sci. 2017;108(10):1947–52.
35. Sumida K, Ohno Y, Ohtake J, Kaneumi S, Kishikawa T, Takahashi N, et al. IL-11 induces differentiation of myeloid-derived suppressor cells through activation of STAT3 signalling pathway. Sci Rep. 2015;15(1):13650.
36. Ohtake J, Kaneumi S, Tanino M, Kishikawa T, Terada S, Sumida K, et al. Neuropeptide signaling through neurokinin-1 and neurokinin-2 receptors augments antigen presentation by human dendritic cells. J Allergy Clin Immunol. 2015;136(6):1690–4.
37. McNab F, Mayer-Barber K, Sher A, Wack A, O'Garra A. Type I interferons in infectious disease. Nat Rev Immunol. 2015;15(2):87–103.
38. Xin L, Vargas-Inchaustegui DA, Raimer SS, Kelly BC, Hu J, Zhu L, et al. Type I IFN receptor regulates neutrophil functions and innate immunity to Leishmania parasites. J Immunol. 2010;184(12):7047–56.
39. Terrazas C, et al. Ly6C^{hi} inflammatory monocytes promote susceptibility to Leishmania donovani infection. Sci Rep. 2017;7(1):14693.
40. Detavernier A, Azouz A, Shehade H, Splittgerber M, Van Maele L, Nguyen M, et al. Monocytes undergo multi-step differentiation in mice during oral infection by *Toxoplasma gondii*. Commun Biol. 2019;2:472.
41. Jones GR, Bain CC, Fenton TM, Kelly A, Brown SL, Ivens AC, et al. Dynamics of colon monocyte and macrophage activation during colitis. Front Immunol. 2018;9:2764.
42. Nguyen A, Ho L, Workenhe ST, Chen L, Samson J, Walsh SR, et al. HDACi delivery reprograms tumor-infiltrating myeloid cells to eliminate antigen-loss variants. Cell Rep. 2018;24(3):642–54.
43. Schouppe E, Mommer C, Movahedi K, Laoui D, Morias Y, Gysemans C, et al. Tumor-induced myeloid-derived suppressor cell subsets exert either inhibitory or stimulatory effects on distinct CD8+ T-cell activation events. Eur J Immunol. 2013;43(11):2930–42.
44. Leon-Cabrera S, Vázquez-Sandoval A, Molina-Guzman E, Delgado-Ramirez Y, Delgado-Buenrostro NL, Callejas BE, et al. Deficiency in STAT1 signaling predisposes gut inflammation and prompts colorectal cancer development. Nat Rev Gastroenterol Cancers. 2018;10(9):341.
45. Zigmond E, et al. Ly6C hi monocytes in the inflamed colon give rise to proinflammatory effector cells and migratory antigen-presenting cells. Immunity. 2012;37(6):1076–90.
46. Tokuyama H, Ueha S, Kurachi M, Matsushima K, Moriyasu F, Blumberg RS, et al. The simultaneous blockade of chemokine receptors CCR2, CCR5 and CXCR3 by a non-peptide chemokine receptor antagonist protects mice from dextran sodium sulfate-mediated colitis. Int Immunol. 2005;17(8):1023–34.
47. Mackos AR, Galley JD, Eubank TD, Easterling RS, Parry NM, Fox JG, et al. Social stress-enhanced severity of *Citrobacter rodentium*-induced colitis is CCL2-dependent and attenuated by probiotic *Lactobacillus reuteri*. Mucosal Immunol. 2016;9(2):515–26.
48. Dai L, Liu Y, Cheng L, Wang H, Lin Y, Shi G, et al. SARI attenuates colon inflammation by promoting STAT1 degradation in intestinal epithelial cells. Mucosal Immunol. 2019;12(5):1130–40.
49. He J, Song Y, Li G, Xiao P, Liu Y, Xue Y, et al. Fbxw7 increases CCL2/7 in CX3CR1hi macrophages to promote intestinal inflammation. J Clin Investig. 2019;129(9):3877–93.
50. Wolf Y, Shemer A, Polonsky M, Gross M, Mildner A, Yona S, et al. Autonomous TNF is critical for in vivo monocyte survival in steady state and inflammation. J Exp Med. 2017;214(4):905–17.
51. Barrow AD, Palarasah Y, Bugatti M, Holehouse AS, Byers DE, Holtzman MJ, et al. OSCAR is a receptor for surfactant protein D

that activates TNF-alpha release from human CCR2+ inflammatory monocytes. J Immunol. 2015;194(7):3317–26.
52. Lamb CA, Kennedy NA, Raine T, Hendy PA, Smith PJ, Limdi JK, et al. British Society of Gastroenterology consensus guidelines on the management of inflammatory bowel disease in adults. Gut. 2019;68:s1–106.
53. Feagan BG, Sandborn WJ, D'Haens G, Panés J, Kaser A, Ferrante M, et al. Induction therapy with the selective interleukin-23 inhibitor risankizumab in patients with moderate-to-severe Crohn's disease: a randomised, double-blind, placebo-controlled phase 2 study. Lancet. 2017;389(10080):1699–709.
54. Sands BE, Sandborn WJ, Panaccione R, O'Brien CD, Zhang H, Johanns J, et al. Ustekinumab as induction and maintenance therapy for ulcerative colitis. N Engl J Med. 2019;381(13):1201–14.
55. Sandborn WJ, Ferrante M, Bhandari BR, Berliba E, Feagan BG, Hibi T, et al. Efficacy and safety of mirikizumab in a randomized phase 2 study of patients with ulcerative colitis. Gastroenterology. 2020;158(3):537-549.e10.
56. Pithadia AB, Jain S. Treatment of inflammatory bowel disease. Pharmacol Rep. 2011;63(3):629–42.
57. Bernstein CN. Treatment of IBD: where we are and where we are going. Am J Gastroenterol. 2015;110(1):114–26.
58. Gisbert JP, Marín AC, Chaparro M. The risk of relapse after anti-TNF discontinuation in inflammatory bowel disease: systematic review and meta-analysis. Am J Gastroenterol. 2016;111(5):632–47.
59. Gaujoux R, Starosvetsky E, Maimon N, Vallania F, Bar-Yoseph H, Pressman S, et al. Cell-centred meta-analysis reveals baseline predictors of anti-TNF alpha non-response in biopsy and blood of patients with IBD. Gut. 2019;68(4):604–14.
60. Cohen BL, Sachar DB. Update on anti-tumor necrosis factor agents and other new drugs for inflammatory bowel disease. BMJ. 2017;357:j2505.